Article

Hydration State of Nonionic Surfactant Monolayers at the Liquid/Vapor Interface: Structure Determination by Vibrational Sum Frequency Spectroscopy

Eric Tyrode, C. Magnus Johnson, Atte Kumpulainen, Mark W. Rutland, and Per M. Claesson

J. Am. Chem. Soc., **2005**, 127 (48), 16848-16859• DOI: 10.1021/ja053289z • Publication Date (Web): 11 November 2005

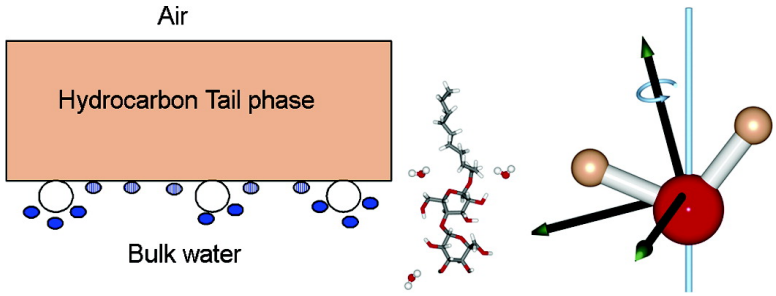

More About This Article

Additional resources and features associated with this article are available within the HTML version:

- Supporting Information
- Links to the 12 articles that cite this article, as of the time of this article download
- Access to high resolution figures
- Links to articles and content related to this article
- Copyright permission to reproduce figures and/or text from this article

View the Full Text HTML

J|A|C|S
ARTICLES
Published on Web 11/11/2005

Hydration State of Nonionic Surfactant Monolayers at the Liquid/Vapor Interface: Structure Determination by Vibrational Sum Frequency Spectroscopy

Eric Tyrode,*,† C. Magnus Johnson,‡ Atte Kumpulainen,† Mark W. Rutland,† and Per M. Claesson†

Contribution from the Department of Chemistry, Surface Chemistry, Royal Institute of Technology, Drottning Kristinas Väg 51, SE-100 44 Stockholm, Sweden, YKI, Institute for Surface Chemistry, Stockholm, Sweden, and Division of Corrosion Science, Royal Institute of Technology, Drottning Kristinas Väg 51, SE-100 44 Stockholm, Sweden

Received May 19, 2005; E-mail: tyrode@kth.se

Abstract: The OH stretching region of water molecules in the vicinity of nonionic surfactant monolayers has been investigated using vibrational sum frequency spectroscopy (VSFS) under the polarization combinations ssp, ppp, and sps. The surface sensitivity of the VSFS technique has allowed targeting the few water molecules present at the surface with a net orientation and, in particular, the hydration shell around alcohol, sugar, and poly(ethylene oxide) headgroups. Dramatic differences in the hydration shell of the uncharged headgroups were observed, both in comparison to each another and in comparison to the pure water surface. The water molecules around the rigid glucoside and maltoside sugar rings were found to form strong hydrogen bonds, similar to those observed in tetrahedrally coordinated water in ice. In the case of the poly(ethylene oxide) surfactant monolayer a significant ordering of both strongly and weakly hydrogen bonded water was observed. Moreover, a band common to all the surfactants studied, clearly detected at relatively high frequencies in the polarization combinations ppp and sps, was assigned to water species located in proximity to the surfactant hydrocarbon tail phase, with both hydrogen atoms free from hydrogen bonds. An orientational analysis provided additional information on the water species responsible for this band.

Introduction

Hydrophobicity is the driving force for self-assembly of amphiphilic compounds into micelles, liquid crystalline phases, and membranes,[1,2] and it is generally the primary motive for adsorption of surfactants at nonpolar interfaces. It is also of paramount importance for protein folding. However, once these structures are assembled, their function in biology and technology is largely determined by interactions occurring at their polar surfaces. Water interacts strongly with these polar surfaces, and thus the involvement of water molecules in surface reactions occurring at biomembrane surfaces, at protein surfaces, and in artificial micellar nanoreactors is expected to be important.[3] Interfacial water next to polar groups is also of importance for the function of "protein repellant" surfaces used for inert coatings in biosensors[4] and for the short-range hydration repulsion between, for example, phospholipid membranes.[5,6] Progress in understanding the role of water for such important surface phenomena that govern biological and technological processes has been slow, largely because there has been very limited direct information on the water structure at such interfaces.

The hydration state of nonionic surfactant headgroups at the air/water interface is of great importance for the monolayer properties and indeed for the performance of a surfactant in general. While charged surfactants are strongly hydrated due to the polarization effect of the ionic headgroup, the hydration of nonionics is far more subtle. Poly(ethylene oxide) surfactants, for example, exhibit a complex interaction with water, which is strongly dependent on the temperature. This leads to phenomena such as clouding of micellar solutions at elevated temperatures and the phase inversion of microemulsion systems.[7,8] While these phenomena are well documented, there is no agreement behind the underlying molecular mechanism.

Sugar-based nonionic surfactants have also received a great deal of attention recently, owing to their superior biodegradability and the fact that the headgroups are obtained from renewable resources. The interaction between water and sugar

† Department of Chemistry, Surface Chemistry, Royal Institute of Technology and YKI, Institute for Surface Chemistry.
‡ Division of Corrosion Science, Royal Institute of Technology.

(1) Tanford, C. *The Hydrophobic Effect: Formation of Micelles and Biological Membranes*, 2nd ed.; Wiley: New York, 1980.
(2) Israelachvili, J. N. *Intermolecular and Surface Forces*; Academic Press: London, 1991.
(3) Levinger, N. E. *Science* **2002**, *298*, 1722−1723.
(4) Gombotz, W. R.; Wang, G.; Horbett, T. A.; Hoffman, A. S. *J. Biomed. Mater. Res.* **1991**, *25*, 1547−1562.
(5) Marra, J.; Israelachvili, J. *Biochemistry* **1985**, *24*, 4608−4618.
(6) Parsegian, V. A.; Fuller, N.; Rand, R. P. *Proc. Natl. Acad. Sci. U.S.A.* **1979**, *76*, 2750−2754.
(7) Shinoda, K.; Arai, H. *J. Phys. Chem.* **1964**, *68*, 3485−3490.
(8) Tiddy, G. J. T. *Phys. Rep.* **1980**, *57*, 3−46.

10.1021/ja053289z CCC: $30.25

groups is of great general interest, not only for understanding surfactant behavior but also for unraveling the role of water in biochemical processes involving carbohydrate units. Hence, much effort has gone into describing sugar/water interactions that are dominated by hydrogen bond formation between water and hydroxyl groups on the sugar unit.[9−11] Since hydrogen bonds are highly directional, it is not surprising that the net interaction depends crucially on the orientation of the hydroxyl groups of the sugar molecule. In fact, changing the direction of one sugar hydroxyl group can make the difference between solubility and nonsolubility. For instance, it is well-known[12] that myoinositol is rather water-soluble whereas scyllo-inositol, which differs only in the orientation of one hydroxyl group, is insoluble. Advances in the comprehension of water/carbohydrate interactions and their relevance for biochemical processes and technical applications require the use of new techniques.

Targeting the aqueous structure at interfaces is not a simple task since many of the techniques that are able to probe these structures lack the necessary surface sensitivity. Vibrational sum frequency spectroscopy (VSFS) represents an ideal choice to study the hydration of nonionic surfactant headgroups adsorbed to the air/water interface, since it is able to distinguish just the few water molecules present at the surface, even in the presence of a vast majority of the same molecules in the bulk. The key property that distinguishes molecules at the surface from those in the bulk is that interfacial molecules have a net polar orientation along the surface normal. Moreover, the vibrational stretching frequency of the OH bond of water, which is the main vibrational mode scrutinized in this report, is known to be very sensitive to the number and strength of hydrogen bonds it forms, red shifting more than 600 cm^{-1} when going from the isolated water molecules in the gas phase to the tetrahedrally coordinated hydrogen-bonded water molecules in ice, as the strength of the OH covalent bond is decreased with increasing strength of the hydrogen bond. VSFS has already been successfully applied to study the pure water liquid/vapor surface,[13] ice/vapor,[14] water/oil,[15] as well as water at solid surfaces such as quartz.[16]

In this article, we use the VSFS technique under three polarization combinations to bear on the issue of the hydration of nonionic surfactant monolayers, focusing primarily on the OH stretching region for various surfactants.

VSFS Principles. In this section, we briefly present the main concepts to readers who may not be familiar with the technique. The full theory behind vibrational sum frequency spectroscopy (VSFS) or sum frequency generation vibrational spectroscopy (SFG-VS) has been described in detail elsewhere.[17−19] Additionally, more comprehensive details about the orientation analysis procedure can be found in other sources.[20−25]

VSFS is a second-order nonlinear optical technique capable of detecting molecules with a net orientation present at any interface accessible by light. Its surface sensitivity resides in the fact that, under the electric dipole approximation, the sum frequency (SF) beam cannot be generated in bulk isotropic media, which is the case for all gases and most liquids and solids. In practice, two pulsed laser beams, one fixed in a visible frequency and the other tunable in the infrared (IR), are directed toward the surface where they are overlapped in time and space. At the interface, in addition to the expected reflections, a third coherent beam having the sum of the frequencies of the two incoming beams is generated. The intensity of the SF radiation which carries the surface information is resonantly enhanced when the IR frequency approaches one of the resonant vibrations of the species present at the surface. Accordingly, the VSF spectra arise from measuring the SF intensity as a function of the IR frequency.

Because of the coherent nature of the sum frequency beam, vibrational modes of nearby or overlapping bands can constructively and/or destructively interfere with each other or with the nonresonant background, causing the VSF spectral profile to be different from those observed in IR or Raman spectroscopy. These interference effects are taken into account when analyzing the spectra.

The SF beam intensity is proportional to the square of the second-order nonlinear susceptibility ($\chi^{(2)}$), the intensity of the IR and visible beams (I_{IR} and I_{vis}), and the square of the Fresnel factors of the corresponding fields (L_{SF}, L_{IR}, and L_{vis}),[23] as shown in eq 1:

$$I_{SFG} \propto |\chi^{(2)}|^2 I_{vis} I_{IR} L_{SF}^2 L_{IR}^2 L_{vis}^2 \quad (1)$$

The Fresnel factors depend on the incident angles of the different beams and the refractive indexes of the interface and bulk phases involved in the SF process. $\chi^{(2)}$ is a third rank tensor of 27 elements that contains the intrinsic surface information. Due to the symmetry constraints at the interface, only a fraction of the elements are independent and nonzero. The actual values of these nonzero elements can be deduced by measuring the spectra using different polarization combinations for the input and output fields. For surfaces that are isotropic in the plane, such as the systems presented in this report, only four of the eight possible polarization combinations give rise to SF signal: ssp, ppp, sps, and pss, where the letters designate the polarization, whether parallel (*p*) or perpendicular (*s*) to the plane of incidence of the SF, visible, and infrared beams, respectively. Far away from electronic resonances, the sps and pss spectra only differ by a constant that is related to the Fresnel factors, and therefore pss spectra will not be shown here, since no additional information can be obtained from them. Collecting spectra at different

(9) Brady, J. W.; Schmidt, R. K. *J. Phys. Chem.* **1993**, *97*, 958−966.
(10) Zuccarello, F.; Buemi, G. *Carbohydr. Res.* **1995**, *273*, 129−145.
(11) Fringant, C.; Tvaroska, I.; Mazeau, K.; Rinaudo, M.; Desbrieres, J. *Carbohydr. Res.* **1995**, *278*, 27−41.
(12) Claesson, P. M. *Surf. Sci. Ser.* **1998**, *75*, 281−320.
(13) Du, Q.; Superfine, R.; Freysz, E.; Shen, Y. R. *Phys. Rev. Lett.* **1993**, *70*, 2313−2316.
(14) Wei, X.; Miranda, P. B.; Zhang, C.; Shen, Y. R. *Phys. Rev. B: Condens. Matter* **2002**, *66*, 085401/085401−085401/085413.
(15) Scatena, L. F.; Brown, M. G.; Richmond, G. L. *Science* **2001**, *292*, 908−912.
(16) Ostroverkhov, V.; Waychunas, G. A.; Shen, Y. R. *Chem. Phys. Lett.* **2004**, *386*, 144−148.
(17) Shen, Y. R. Surface spectroscopy by nonlinear optics. In *Frontiers in Laser Spectroscopy*, Proceedings of the International School of Physics "Enrico Fermi", Varenna on Lake Como, Villa Monastero, Italy, June 23−July 3, 1992; Hänsch, T. W., Inguscio, M., Eds.; Elsevier: Amsterdam, 1994; pp 139−165.
(18) Bain, C. D. *Surf. Sci. Ser.* **1999**, *83*, 335−373.
(19) Richmond, G. L. *Chem. Rev.* **2002**, *102*, 2693−2724.
(20) Hirose, C.; Akamatsu, N.; Domen, K. *Appl. Spectrosc.* **1992**, *46*, 1051−1072.
(21) Hirose, C.; Yamamoto, H.; Akamatsu, N.; Domen, K. *J. Phys. Chem.* **1993**, *97*, 10064−10069.
(22) Bell, G. R.; Li, Z. X.; Bain, C. D.; Fischer, P.; Duffy, D. C. *J. Phys. Chem. B* **1998**, *102*, 9461−9472.
(23) Zhuang, X.; Miranda, P. B.; Kim, D.; Shen, Y. R. *Phys. Rev. B: Condens. Matter* **1999**, *59*, 12632−12640.
(24) Lu, R.; Gan, W.; Wu, B.-H.; Chen, H.; Wang, H.-F. *J. Phys. Chem. B* **2004**, *108*, 7297−7306.
(25) Tyrode, E.; Johnson, C. M.; Baldelli, S.; Leygraf, C.; Rutland, M. W. *J. Phys. Chem. B* **2005**, *109*, 329−341.

polarization combinations can be used to extract information regarding the orientation of specific bonds at the surface, as well as identifying all possible molecular species present at the studied interface, since some vibrational modes may be very weak or not observable in a certain polarization combination but evident in others, due to the symmetry of the mode and/or orientational arguments.

To understand the molecular origin of the SF response, $\chi^{(2)}$ can be divided into two contributing terms: a nonresonant contribution from the substrate ($\chi^{(2)}_{NR}$), which for our particular case is a real constant, and a second term that includes the sum of the resonant contributions to $\chi^{(2)}$ from the n vibrational modes of the interfacial molecules ($\chi^{(2)}_{R,n}$), according to eq 2:

$$\chi^{(2)} = \chi^{(2)}_{NR} + \sum_n \chi^{(2)}_{R,n} \quad (2)$$

$\chi^{(2)}_{R,n}$ is proportional to the number of molecules, N, and the orientationally averaged molecular hyperpolarizability for the vibrational resonance $\langle\beta^{(2)}_n\rangle$, as described in eq 3:

$$\chi^{(2)}_{R,n} = \frac{N}{\epsilon_0}\langle\beta^{(2)}_n\rangle \quad (3)$$

where ϵ_0 is the dielectric permittivity. $\beta^{(2)}_n$ is usually expressed in molecular coordinates ($\alpha,\beta,\gamma = a,b,c$) and is related to the Raman tensor elements ($\alpha_{\alpha\beta}$) and the IR transition moment (μ_γ), according to eq 4:

$$\beta^{(2)}_{\alpha\beta\gamma,n} = \frac{\alpha_{\alpha\beta,n}\,\mu_{\gamma,n}}{\omega_n - \omega_{IR} - i\Gamma_n} \quad (4)$$

where ω_{IR} is the frequency of the infrared laser beam, ω_n is the vibrational transition frequency, i is the imaginary unit, and Γ_n is the damping constant. From eq 4 it is clear that vibrational modes are only SF active if they are both IR and Raman active. The transformation of the molecular hyperpolarizability $\beta^{(2)}_n$ in molecular coordinates (α,β,γ) to the second-order susceptibility $\chi^{(2)}_{R,n}$ in surface coordinates (x,y,z) is carried out through an Euler rotational transformation matrix.[20] The average orientation of the molecule is given in terms of the Euler angles: χ (azimuthal angle), θ (tilt), and ϕ (twist), which represent the rotation of the molecular axes (α,β,γ) with respect to surface fixed axes (x,y,z), where z is the surface normal.

The theoretical predictions of the VSF spectra, and the corresponding orientation analysis, could in principle be calculated if the $\beta^{(2)}_n$ elements are known. The number of nonvanishing elements of $\beta^{(2)}_n$ can be identified considering the molecular symmetry of the nth vibrational mode, while the actual values can be explicitly determined from the IR transition moment vector and the Raman tensor elements.

Experimental Procedures

The VSFS experimental setup has already been described in detail elsewhere.[26] Briefly, a Nd:YAG 1064-nm picosecond laser (EKSPLA) is used to pump an OPG/OPA (LaserVision), where the visible (532 nm) and tunable IR laser beams are generated. In this experiment, the IR beam was tuned from 2600 to 4000 cm^{-1} with an average energy per pulse at the surface ranging from 150 to 300 μJ (bandwidth $\approx$ 8 cm^{-1}). The energy of the visible beam was ~0.9 mJ/pulse with a beam diameter of approximately 1.4 mm at the sample surface. The beams are overlapped at the sample surface using a copropagating reflection geometry with incidence angles of 55° and 63° for the visible and IR beams, respectively. The liquid sample to be analyzed is placed in a sealed glass/Teflon cell designed for this purpose, with an overhead space for IR absorption normalization. The generated SF beam is first spatially filtered, passed through a monochromator, and finally detected with a photomultiplier tube (PMT). The signal is then processed in an integrated boxcar and registered in a PC using a LabVIEW program. Spectra at the different polarization combinations studied in this report were gathered successively by rotating the halfwave plates for the IR and visible beams, respectively, and the polarizer for the SF beam. Spectra were also normalized to account for polarization and wavelength dependence of the band-pass filter, Notch Plus filter, monochromator, and PMT. The experiments were repeated on at least three different occasions.

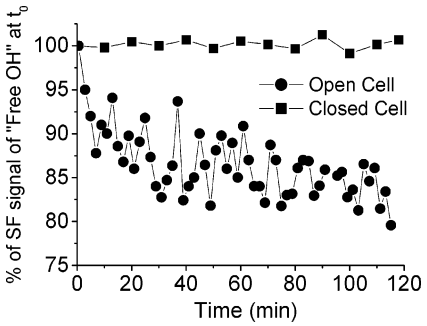

Figure 1. Variation of the water surface SF intensity at 3702 cm^{-1} of the free OH in the ssp polarization combination as a function of time, in a cell open to laboratory air and in a closed cell. The ordinate is expressed as the percentage of the full SF signal at time 0. These experiments were carried out at 3 °C with the aim to reduce evaporation in the open cell.

The cleanness of the measuring vessel was found to be of particular importance, as minute amounts of contaminants are sufficient to foul the liquid surface. Before each measurement, the cell was cleaned with a mixture of concentrated nitric and sulfuric acid and left standing for at least 24 h. The cell was subsequently rinsed with copious amounts of Milli-Q water, following various flushing cycles over several days. In the final rinsing stage the surface tension and pH were measured and found to comply with the expected values for pure water. Similar results were obtained using commercially available alkaline cleaning agents such as Clean-X (Goteborgs Termometerfabrik AB).

At this stage, it is worth noting the importance of performing the experiments in a closed cell, not only for correcting for the absorption of the IR beam before reaching the sample's surface, but in particular to avoid contamination of the high energy surface of pure water by airborne contaminants (e.g., oil/dust). In Figure 1, the fluctuations of the intensity of the SF signal for the "free OH" at 3702 cm^{-1} are shown as a function of time in a cell open to the laboratory air. In this measurement, each point is an average of 3000 shots normalized for IR and visible beam power fluctuations. The evident drop in the intensity measured is a consequence of the adsorption of contaminants from the surrounding air, while the increased scattering in the experimental data is explained in terms of contaminants moving in and out of the probing area. Considerably higher signal losses can be obtained in the same time scale under slightly different laboratory conditions (e.g., humid conditions). For comparison, the normalized "free OH" intensity is also shown in Figure 1 for our closed cell, which has been found to be constant to within less than 5% even after more than 40 h of continuous experiments. Considering that on average 4 h were needed to collect each of the spectra presented here shows that a closed cell is not only desirable, but necessary.

Chemicals. 1-Decanol was obtained from Fluka (puriss ≥99.5% GC) and used as received. The surfactants *n*-decyl-β-D-glucopyranoside and

(26) Johnson, C. M.; Tyrode, E.; Baldelli, S.; Rutland, M. W.; Leygraf, C. *J. Phys. Chem. B* **2005**, *109*, 321−328.

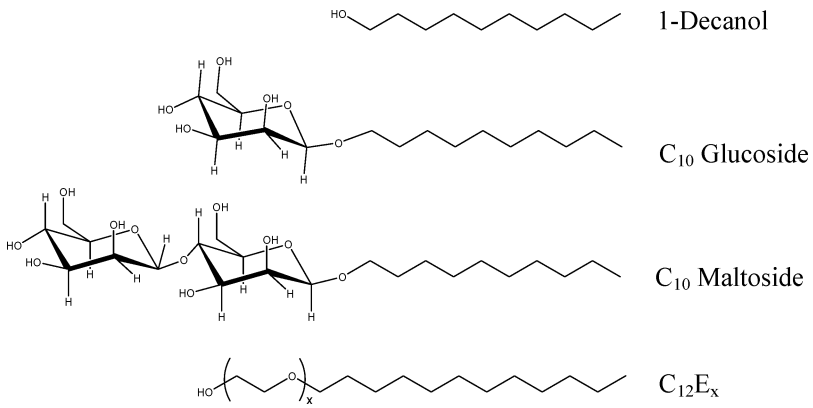

Figure 2. Molecular structures of the surfactants studied in this article. The abbreviations used in the text are shown next to each structure. The *x* in the $C_{12}E_x$ case was either 4 or 8.

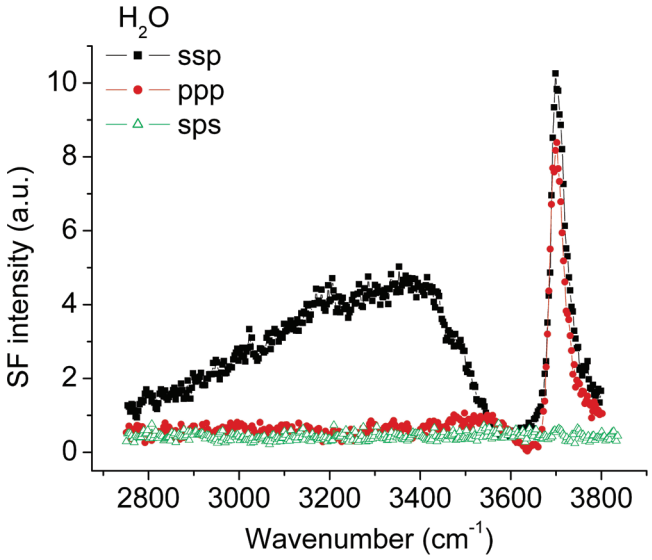

Figure 3. VSF spectra for pure water at the liquid/vapor interface in the polarization combinations ssp, ppp, and sps. The lines are guides to the eye, joining consecutive data points.

n-decyl-β-D-maltopyranoside, hereafter referred to as C_{10}Glucoside and C_{10}Maltoside, were used as received from Sigma (>98% GC) and Anatrace (Anagrade), respectively. The tetra(ethylene oxide) *n*-dodecyl ether ($C_{12}E_4$) and octa(ethylene oxide) *n*-dodecyl ether ($C_{12}E_8$) were obtained from Nikkol and also used without further purification. The molecular structures of these components are shown in Figure 2. The 1-decanol monolayer was prepared by placing a drop on the surface water as described previously.[27]

The water used in the experiments was obtained from a Millipore RiOs-8 and Milli-Q PLUS 185 purification system, finally filtered through a 0.2 μm Millipak filter. The resistivity was 18.2 MΩ/cm, while the total organic carbon content of the outgoing water was monitored with a Millipore A-10 unit and did not exceed 6 ppb during any of the measurements.

Results and Discussion

The Pure Water Surface. Figure 3 shows the SF spectra of pure water using the ssp, ppp, and sps polarization combinations in the OH stretching region. The SF spectra from the surface of pure water serve as a reference for measurements in water/solute mixtures and will be described in this section. The ssp spectrum agrees with spectra previously reported.[13,26,28−30] The main features are a broad band extending for a few hundred wavenumbers in the low frequency range, followed by a sharp peak centered at approximately 3700 cm^{-1}. This last narrow and strong peak, usually referred to as "free OH" or "dangling OH" in the SF literature, is situated close in frequency to the uncoupled OH stretching vibration in gas-phase HDO monomers (IR[31] and Raman[32] at 3707 cm^{-1}) and between the symmetric ν_1 (IR[31] and Raman[32] at 3657 cm^{-1}) and asymmetric ν_3 (IR[31] and Raman[32] at 3756 cm^{-1}) stretch of gas-phase H_2O. It has been unambiguously assigned to the uncoupled OH stretching mode of surface water molecules with one OH bond protruding out into the gas phase, vibrating unrestrained from hydrogen bonds. The water molecules contributing to this peak must necessarily be present at the top monolayer of the liquid/vapor interface.

On the other hand, the intensity observed below 3600 cm^{-1} is in general terms attributed to hydrogen-bonded water molecules of varying strength and coordination, both properties being greater at lower frequencies (lower wavenumbers). It has been theoretically deduced that 90% of the intensity of this band stems from water species present in the first two monolayers.[33] The detailed assignment of the water species contributing to this band is less straightforward, and several attempts to identify them have been performed. The simplest approach has been to separate the band into two broad peaks[13,19,34] centered at ~3200 cm^{-1} and at ~3450 cm^{-1}, loosely referred to as stronger hydrogen-bonded and weaker hydrogen-bonded peaks, respectively. The former is also called "icelike", due to its closeness in frequency to the OH stretching mode of tetrahedrally coordinated water molecules at the surface of ice[14] (~3150 cm^{-1}). It is clear, however, that different species of water with an overall symmetric character[33] contribute to this "strongly hydrogen-bonded" band. This band also includes the other uncoupled OH oscillator,[29,34−36] which is intramolecularly

(27) Braun, R.; Casson, B. D.; Bain, C. D. *Chem. Phys. Lett.* **1995**, *245*, 326−334.
(28) Wei, X.; Shen, Y. R. *Phys. Rev. Lett.* **2001**, *86*, 4799−4802.
(29) Liu, D.; Ma, G.; Levering, L. M.; Allen, H. C. *J. Phys. Chem. B* **2004**, *108*, 2252−2260.
(30) Raymond, E. A.; Richmond, G. L. *J. Phys. Chem. B* **2004**, *108*, 5051−5059.
(31) Shimanouchi, T. *Tables of Molecular Vibrational Frequencies Consolidated*; National Bureau of Standards: New York, 1972; Vol. I.
(32) Avila, G.; Fernandez, J. M.; Tejeda, G.; Montero, S. *J. Mol. Spectrosc.* **2004**, *228*, 38−65.
(33) Morita, A.; Hynes, J. T. *Chem. Phys.* **2000**, *258*, 371−390.
(34) Shultz, M. J.; Baldelli, S.; Schnitzer, C.; Simonelli, D. *J. Phys. Chem. B* **2002**, *106*, 5313−5324.

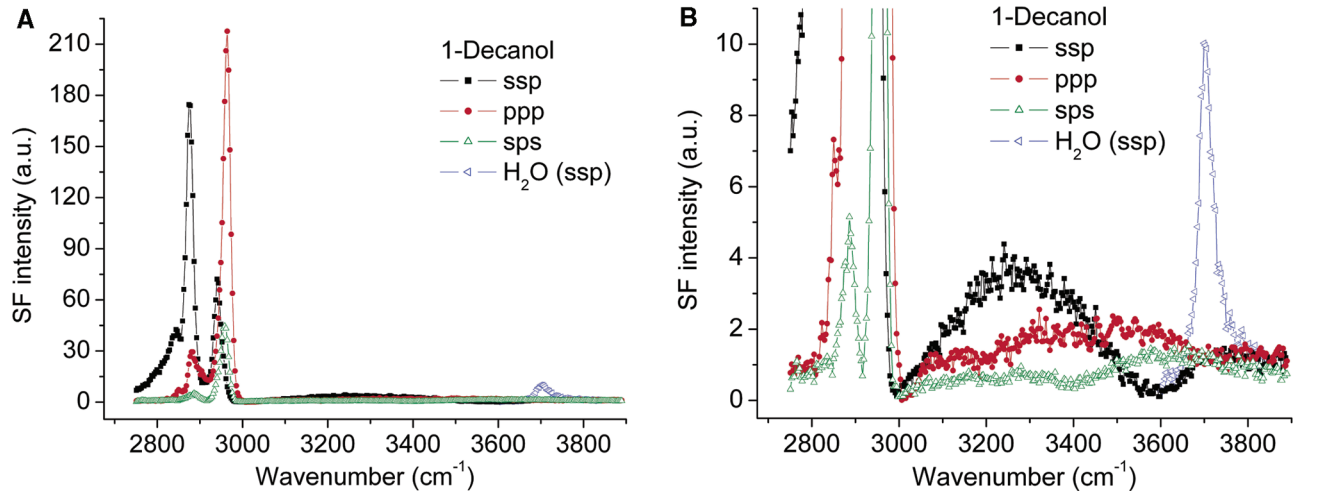

Figure 4. (a) Full scale VSF spectra for a saturated solution of 1-decanol at 20 °C for ssp, ppp, and sps polarization combinations. (b) Enlarged scale of the SF intensity to facilitate the examination of the OH stretching region for decanol and water. The "free OH" peak of pure water under ssp polarization combination is shown as a reference. The lines are guides to the eye joining consecutive data points.

adjacent to the free OH but directed toward the liquid bulk phase, participating in hydrogen bonding with neighboring water molecules. In contrast, the weaker hydrogen-bonded peak at higher frequencies, typically labeled as "liquidlike" in analogy to the position of the strongest band observed in bulk Raman spectra of liquid water,[37] is associated with molecules vibrating in a more disordered hydrogen-bonded network.

Other approaches,[29,30,38] also based on IR and Raman studies, separate the broad hydrogen-bonded peak into three or more contributing bands. Obviously, increasing the number of peaks provides a better fitting of the experimental data; however, we believe that there is no physical insight to be gained in the present work through attempting to apply such a method.

Another feature commonly observed[29,30,39] in the ssp spectrum of pure water on the high-frequency side of the free OH ($\sim$3760 cm^{-1}), originally ascribed to the asymmetric stretch of oriented water vapor, is not observed in any of our measurements. However, we note that such a feature appears in the spectra if the IR normalization from the gas-phase absorption is ignored. This is due to the strong and sharp absorption of the IR laser beam from the rovibrational bands of water in the gas phase, in particular the asymmetric stretch at 3756 cm^{-1}.

The ppp and sps polarization combinations for pure water are also presented in Figure 3. Both are consistent with previous studies.[25,28] Similar to ssp, the ppp spectrum shows a sharp peak at 3702 cm^{-1} assigned to the "free OH". On the other hand, no SF intensity is observed in the hydrogen-bonded region, in addition to a weak feature centered at $\sim$3550 cm^{-1}, which due to its relative high frequency is assigned to OH bonds only weakly perturbed by hydrogen bonding to neighbors. Finally, no evident resonant features are observed in the sps spectrum in the entire OH stretching range. As discussed in the theory section, collecting spectra at the different polarization combinations can be used to extract information regarding the orientation of specific bonds at the surface. The tilt angle of the "free OH" bond has been calculated to be close to 35° from the surface normal.[13,25] The lack of prominent features in the lower frequency side of the ppp and sps water spectra is linked to the specific orientation and molecular symmetry of the vibrational modes of the different water species, which are responsible for the broadband in the ssp spectrum. This will be discussed in more detail in the Orientational Analysis section.

Surfactant Systems. Upon addition of a surface active compound, the surface of water is quickly perturbed. For surfactant systems, the free OH peak characteristic of the neat water surface completely disappears once the liquid-expanded surfactant phase is formed at the air/liquid interface,[40] which is usually 1 or 2 orders of magnitude below the critical micelle concentration (cmc). The liquid-expanded phase can be thought of as a very thin liquid film where the hydrocarbon tails are in a random liquidlike configuration. This normally represents the final state of adsorption of soluble surfactants as the monolayer state does not change much after the cmc. The presence of the surfactant can also be traced by targeting the stretching frequencies of its characteristic groups. For surfactants with hydrocarbon tails, the typical vibrational modes examined are the CH stretching vibrations, which can be used not only to identify their existence at the surface but also to extract information of their relative orientation and order as developed below.

Decanol. Decanol, as well as longer chain fatty alcohols, forms a densely packed and highly conformationally ordered monolayer at the vapor/water interface. Experiments were performed at 20 °C, which is above the two-dimensional melting point of decanol ($T_{m2D} \approx 14.3$ °C), where a phase transition toward a liquid-expanded phase with a change in molecular area from 21.5 to 24 Å^2 is observed.[41] In Figure 4a, the VSF spectra of decanol under different polarization combinations are shown, where the sharp and strong peaks from the CH stretching vibrations between 2800 and 3000 cm^{-1} are obvious. The

(35) Steinbach, C.; Andersson, P.; Kazimirski, J. K.; Buck, U.; Buch, V.; Beu, T. A. *J. Phys. Chem. A* **2004**, *108*, 6165−6174.
(36) Walrafen, G. E. *J. Chem. Phys.* **2004**, *120*, 4868−4876.
(37) Carey, D. M.; Korenowski, G. M. *J. Chem. Phys.* **1998**, *108*, 2669−2675.
(38) Raymond, E. A.; Tarbuck, T. L.; Brown, M. G.; Richmond, G. L. *J. Phys. Chem. B* **2003**, *107*, 546−556.
(39) Brown, M. G.; Raymond, E. A.; Allen, H. C.; Scatena, L. F.; Richmond, G. L. *J. Phys. Chem. A* **2000**, *104*, 10220−10226.
(40) Kumpulainen, A. J.; Persson, C. M.; Eriksson, J. C. *Langmuir* **2004**, *20*, 10935−10942.
(41) Berge, B.; Konovalov, O.; Lajzerowicz, J.; Renault, A.; Rieu, J. P.; Vallade, M.; Als-Nielsen, J.; Gruebel, G.; Legrand, J. F. *Phys. Rev. Lett.* **1994**, *73*, 1652−1655.

assignments in this range are well established:[27,42−44] the peaks at 2877 and 2944 cm^{-1} in the ssp spectrum arise, respectively, from the symmetric methyl stretch (r^+) and its Fermi resonance with an overtone of the methyl bending mode (r^+_{FR}). The methylene symmetric stretch (d^+) is only observed as a shoulder at ∼2850 cm^{-1}, indicating a small number of gauche defects. In an all-trans hydrocarbon chain configuration, the methylene groups are in a locally centrosymmetric environment, effectively rendering the CH_2 vibrations SF inactive. The ratio between the fitted r^+ and d^+ amplitudes has been proposed as a useful indicator of the degree of conformational order in the monolayer,[42] which for decanol is obviously large. On the other hand, the ppp and sps spectra are dominated by a sharp peak centered at 2965 cm^{-1} assigned to the asymmetric methyl stretch. Moreover, a shoulder observed at ∼2905 cm^{-1} in the ppp spectrum is assigned to the CH_2 asymmetric stretch in accordance with recent VSFG studies of short chain diols.[24]

The OH stretching region is, however, the focus of the current discussion, and henceforth all spectra will be scaled to examine this region in detail. In Figure 4b, the features corresponding to the OH stretching resonant vibrations are now evident for decanol and water. The free OH spectrum of pure water, which was collected at the beginning of each experiment, will be shown as a reference for the spectra of each surfactant. The intensities observed correspond to water molecules with a preferred orientation in close proximity to the surfactant's uncharged headgroup and hydrocarbon tail. Since decanol, like all the other surfactants investigated in this study, is nonionic, no enhancement of the VSF signal due to an electrostatic surface field is expected. This surface field is known[16,45,46] to induce an enhanced ordering of the interfacial water molecules, which can extend over several molecular layers, increasing the nonlinearity of the surface layer and, as a consequence, also the probing depth. The lack of surface charge permits the examination of the orientation of water molecules affected by weaker and shorter range interactions.

In comparison to pure water (Figure 3), the ssp spectrum of Figure 4b shows significant variations, clearly reflecting the difference between the neat water surface and the aqueous layer below the decanol monolayer. On the basis of a VSF report on pure short-chain alcohols,[47] the band centered at ∼3250 cm^{-1}, which overlaps with the water vibrations, is assigned primarily to the OH stretching of the hydrogen-bonded decanol's hydroxyl group. We nonetheless suggest that since water molecules are necessarily hydrating the decanol hydroxyl group which has a preferred orientation, they also contribute to this intensity through strongly hydrogen-bonded (hydration) water coupled to the surfactant headgroup. This band can also be seen in the other two polarization combinations.

However, in the ppp and particularly in the sps spectrum the dominant intensity in the OH stretching range appears at appreciably higher frequencies (∼3600 cm^{-1}). This band is absent at the pure water surface, and therefore the water species responsible for this intensity must be due to the presence of the surfactant. As discussed in the Introduction, the resonant frequencies of the OH stretching vibrations of water are very sensitive to the number and strength of hydrogen bonds formed with neighboring molecules. In bulk Raman studies[37,48,49] it is generally agreed to consider intensity components above 3500 cm^{-1} as non-hydrogen bonded, and initially we will loosely refer to this band as "non-hydrogen bonded", though it is important to make the distinction with the uncoupled free OH vibrations observed at higher frequencies in both the vapor/water and oil/water[15] interfaces.

We claim that the water molecules responsible for this band are in direct contact with the hydrocarbon surfactant tails which constitute the liquid-expanded phase. Recent vibrational sum frequency studies[15,50] at the hydrocarbon/H_2O and CCl_4/H_2O interfaces have shown enhanced resonant features in the high frequency region of the OH stretching vibrations, leading to the conclusion that the hydrogen bonding between adjacent water molecules close to these interfaces is weak despite being oriented. This statement is consistent with our assertion regarding the origin of the "non-hydrogen band", in the sense that water close to fluid hydrophobic surfaces does not form strong hydrogen bonds, in contrast to what was initially suggested by accepted models of water next to fluid hydrophobic surfaces.[51] In our model, a distinction is made between the water molecules from the hydration shell of the surfactant headgroup and those in direct proximity to the hydrocarbon tails.

The formal separation of the surfactant molecules in a liquid-expanded phase into a liquidlike hydrocarbon tail layer and a second layer where headgroups and water mix in which our model is based has been proven to account well for the free energy contributions of the headgroup layer.[52,53] This model was initially proposed by Langmuir[54] and further developed by Eriksson and Ljunggren.[55]

Similar spectroscopic features are expected from other nonionic surfactants at concentrations sufficiently high to form the liquid-expanded phase. With a view to verifying this assertion, the data from other nonionic systems consisting of sugar and ethylene oxide headgroups can be examined. These molecules are known to form less ordered monolayers with a significantly higher number of gauche defects than those found for decanol due to the lower adsorption.[42] The molecular areas at the cmc together with the value of the cmc are collected in Table 1.

Sugar Surfactants. Figure 5a shows the VSF spectra of C_{10}-Glucoside at a concentration just above the cmc under the polarization combinations ssp, ppp, and sps. The partly truncated peaks on the low-frequency side (2800−3000 cm^{-1}) correspond to the CH stretching vibrations of the hydrocarbon tail, though contributions from the headgroup are also observed, but this will not be discussed further here. The attention is focused on the OH stretching region starting from 3000 cm^{-1}, where in

(42) Bell, G. R.; Bain, C. D.; Ward, R. N. *J. Chem. Soc., Faraday Trans.* **1996**, *92*, 515−523.
(43) Casson, B. D.; Bain, C. D. *J. Phys. Chem. B* **1998**, *102*, 7434−7441.
(44) Sefler, G. A.; Du, Q.; Miranda, P. B.; Shen, Y. R. *Chem. Phys. Lett.* **1995**, *235*, 347−354.
(45) Gragson, D. E.; McCarty, B. M.; Richmond, G. L. *J. Am. Chem. Soc.* **1997**, *119*, 6144−6152.
(46) Miranda, P. B.; Du, Q.; Shen, Y. R. *Chem. Phys. Lett.* **1998**, *286*, 1−8.
(47) Stanners, C. D.; Du, Q.; Chin, R. P.; Cremer, P.; Somorjai, G. A.; Shen, Y. R. *Chem. Phys. Lett.* **1995**, *232*, 407−413.
(48) Walrafen, G. E. *J. Chem. Phys.* **1967**, *47*, 114−126.
(49) Walrafen, G. E. *J. Chem. Phys.* **1971**, *55*, 768−792.
(50) Brown, M. G.; Walker, D. S.; Raymond, E. A.; Richmond, G. L. *J. Phys. Chem. B* **2003**, *107*, 237−244.
(51) Linse, P. *J. Chem. Phys.* **1987**, *86*, 4177−4187.
(52) Persson, C. M.; Jonsson, A. P.; Bergstrom, M.; Eriksson, J. C. *J. Colloid Interface Sci.* **2003**, *267*, 151−154.
(53) Persson, C. M.; Kjellin, U. R. M.; Eriksson, J. C. *Langmuir* **2003**, *19*, 8152−8160.
(54) Langmuir, I. *J. Chem. Phys.* **1933**, *1*, 756−776.
(55) Eriksson, J. C.; Ljunggren, S. *Colloids Surf.* **1989**, *38*, 179−203.

Table 1. Molecular Areas and Critical Micellar Concentrations (cmc) of the Surfactants Used

surfactant	cmc	Å²/molecule	ref
decanol[a]	0.234 mM solubility at 25 °C	24	41, 56
C_{10}Glucoside	2.0 mM at 22 °C	37	57
C_{10}Maltoside	2.2 mM at 22 °C	48	57
C12E4	0.05 mM at 23 °C	42	58
C12E8	0.10 mM at 25 °C	62	59

[a] Decanol does not form micelles in solution.

the ssp spectra a band at ~3150 cm^{-1} is observed. The assignment of this peak is not trivial, since the OH stretches of the glucoside group observed in IR[60] and Raman[61] overlap with the stretching vibrations of water. Nonetheless, the fact that this band appears at such a low frequency is indicative of strong icelike hydrogen bonds of both the water and sugar group. This intensity is then directly linked to the hydroxyl groups of the surfactant headgroup and its hydration shell.

Of particular interest in the ppp and sps spectra of Figure 5a is the band observed at approximately 3590 cm^{-1}, which is absent in the ssp spectrum. Similar to the decanol case, this band is also assigned to water molecules with their hydrogen atoms vibrating free from hydrogen bonds, in close proximity to the hydrocarbon tails. The small red shift would imply somewhat stronger interactions with neighboring molecules.

Comparing the absolute intensities of this "non-hydrogen-bonded" band observed in the spectra of decanol and C_{10}-Glucoside, it can be seen that it is slightly lower for the latter case. As a first approximation the reduced intensity could be related to a decrease in the number of water molecules in contact with the surfactant tails. The larger area per molecule (Table 1) would imply that more water could be accommodated between the headgroups, which seems apparently contradictory. However, it is also important to take into account the size of the headgroup itself. The bulky glucosidic ring of the sugar surfactant acts as an effective shield, reducing the available contact area between the water and the hydrocarbon tails and decreasing the intensity of the band.

In Figure 5b, the equivalent VSF spectra for C_{10}Maltoside are shown. There is a very close resemblance to the C_{10}-Glucoside spectra, though the absolute intensities vary. The increase in the intensity of the peaks partly displayed in the CH stretching region is mainly due to the additional CH groups present at the surfactant headgroup and will be discussed in detail in a future publication. The band centered at 3150 cm^{-1} in the ssp spectrum is ascribed, as for the C_{10}Glucoside, to the OH stretching vibrations of the hydroxyl groups from the sugar rings and the spectral indistinguishable hydration shell, where particularly strong and well coordinated hydrogen bonds are formed. The higher intensity of this band is attributed to an increase in the number of hydroxyl groups and associated H_2O molecules from the hydration shell, implying that both sugar units must have a preferred orientation.

In the ppp and sps spectra of Figure 5b, the strong broad band centered at around 3580 cm^{-1} is found in very much the same position as the one observed for the C_{10}Glucoside. It is also assigned to the OH stretch of water molecules in close proximity to the hydrocarbon tails. The stronger intensity of this band can be explained in terms of the higher number of contributing water molecules, which in turn can be rationalized by the larger area per molecule of the C_{10}Maltoside (Table 1) and the fact that because of steric constraints the second sugar ring is on average directed away from the surface.[62] As a consequence, despite having a bulkier headgroup, there is a net enlargement in the area of contact between water molecules and the hydrocarbon tails compared to the C_{10}Glucoside.

Reducing the concentration of the surfactant solution below its cmc allows the area per molecule to be decreased without changing the headgroup. As will be shown in a future publication, the "non-hydrogen-bonded" band follows the expected behavior in the liquid-expanded region, increasing in intensity at lower concentrations. Experiments were also performed with C_{12}Maltoside (spectra not shown), and the effect of increasing the chain length of the hydrocarbon tail proved to be negligible in the OH stretching range of the spectra of the two maltoside surfactants.

Alkyl Poly(ethylene oxide) Surfactants. Parts a and b of Figure 6 show the VSF spectra of $C_{12}E_4$ and $C_{12}E_8$, both at concentrations just above their respective cmc's. The CH stretching region has been carefully studied by Goates et al.[63] in the ssp polarization combination, and the reader is referred to this work for more detailed information. Useful information for the current discussion can be extracted; for example, the number of gauche defects in the hydrocarbon chain is lower for the $C_{12}E_4$ monolayer. This can be directly linked to the higher surface density achieved at the cmc (Table 1), since it has been shown that the number of ethylene oxide units at a fixed area per molecule does not, per se, affect the structure of the hydrocarbon tails.[63]

On the other hand, the VSF spectra in the OH stretching region of Figure 6a,b are of particular interest, since they add unique information to a long heated debate regarding the structure of water around poly(ethylene oxide) groups.[64−69] In the ssp spectra a broad and strong band extending from 3000 to ~3500 cm^{-1} is observed. This intensity is assigned to the OH stretching of water molecules hydrating the poly(ethylene oxide) headgroup (the contribution from the terminal hydroxyl group of the EO chain to this band is thought to be minute because of the random orientation at the end of the chain[70]). As for the pure water surface, the detailed analysis of the number of water species contributing to this band is not straightforward, though it is clear that the structures at the two surfaces are considerably different. Nonetheless, the broad band in the ssp spectra can be separated into two main contributing peaks centered at ~3250 cm^{-1} and ~3400 cm^{-1}, which are almost

(56) Kinoshita, K.; Ishikawa, H.; Shinoda, K. *Bull. Chem. Soc. Jpn.* **1958**, *31*, 1081−1082.
(57) Persson, C. M.; Kumpulainen, A. J.; Eriksson, J. C. *Langmuir* **2003**, *19*, 6110−6114.
(58) Kjellin, U. R. M.; Claesson, P. M.; Linse, P. *Langmuir* **2002**, *18*, 6745−6753.
(59) Lu, J. R.; Li, Z. X.; Thomas, R. K.; Binks, B. P.; Crichton, D.; Fletcher, P. D. I.; McNab, J. R.; Penfold, J. *J. Phys. Chem. B* **1998**, *102*, 5785−5793.
(60) Rozenberg, M.; Loewenschuss, A.; Marcus, Y. *Carbohydr. Res.* **2000**, *328*, 307−319.
(61) Kacurakova, M.; Mathlouthi, M. *Carbohydr. Res.* **1996**, *284*, 145−157.
(62) Persson, C. M.; Kumpulainen, A. J. *Colloids Surf., A* **2004**, *233*, 43−49.
(63) Goates, S. R.; Schofield, D. A.; Bain, C. D. *Langmuir* **1999**, *15*, 1400−1409.
(64) Goldstein, R. E. *J. Chem. Phys.* **1984**, *80*, 5340−5341.
(65) Matsuyama, A.; Tanaka, F. *Phys. Rev. Lett.* **1990**, *65*, 341−344.
(66) de Gennes, P.-G. *C. R. Acad. Sci. Paris* **1991**, *313*, 1117−1122.
(67) Bekiranov, S.; Bruinsma, R.; Pincus, P. *Europhys. Lett.* **1993**, *24*, 183−188.
(68) Kjellander, R. *J. Chem. Soc., Faraday Trans. 2* **1982**, *78*, 2025−2042.
(69) Karlström, G. *J. Phys. Chem.* **1985**, *89*, 4962−4964.

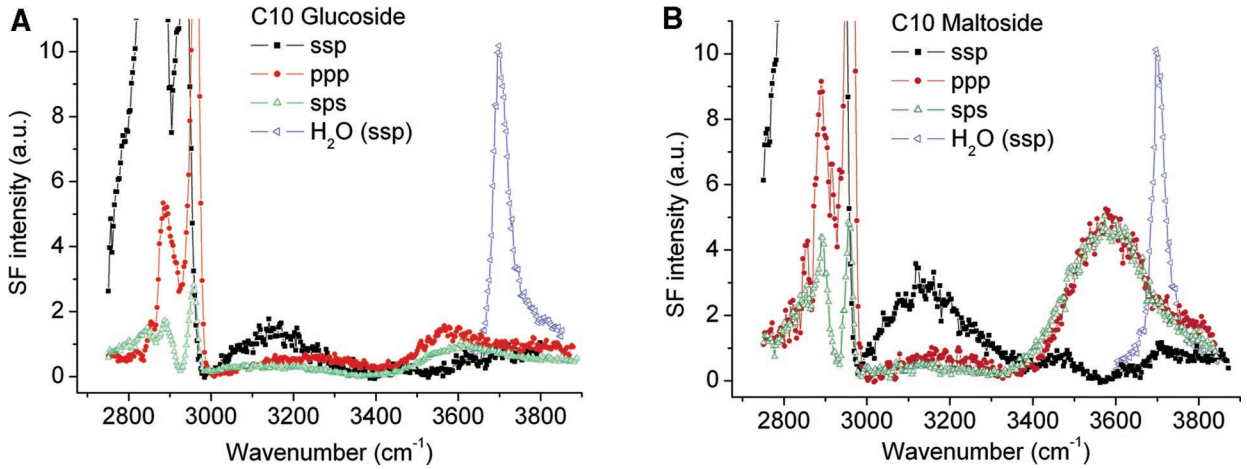

Figure 5. (a) VSF spectra for the polarization combinations ssp, ppp, and sps of an aqueous solution 2.6 mM of C_{10}Glucoside at 22 °C. (b) C_{10}Maltoside at a concentration of 2.6 mM and 22 °C. The "free OH" peak of pure water under ssp polarization combination is also shown for reference. The lines are guides to the eye.

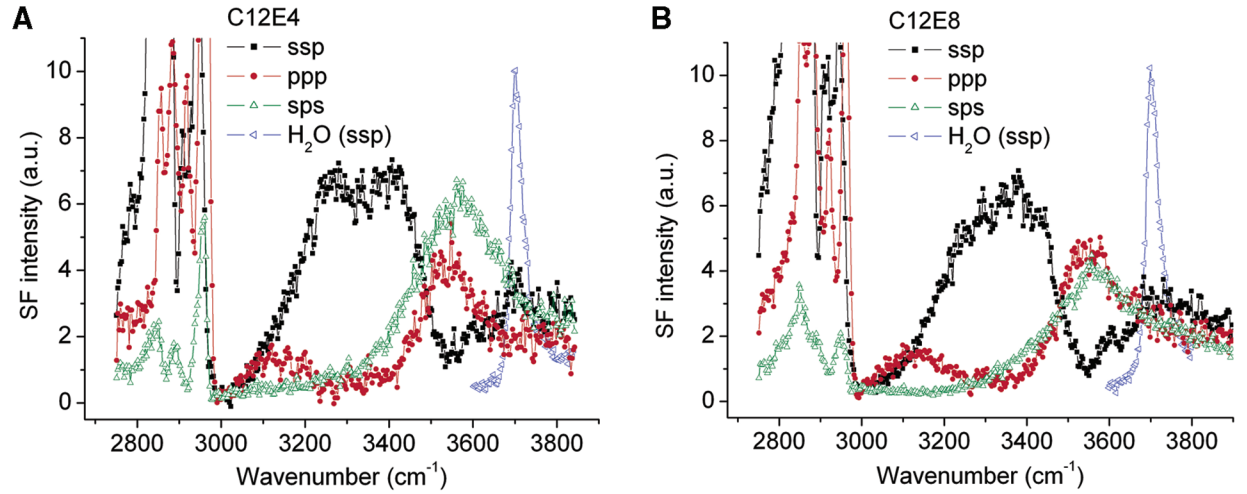

Figure 6. (a) VSF spectra for the polarization combinations ssp, ppp, and sps of an aqueous solution 0.15 mM of $C_{12}E_4$ at 20 °C. (b) $C_{12}E_8$ at a concentration of 0.33 mM and 20 °C. The "free OH" peak of pure water under ssp polarization combination is also shown for reference. The lines are guides to the eye.

discernible in the spectra of Figure 6. As mentioned before, the degree of red shifting reflects the strength and coordination of the water molecules, and it seems that for the ssp polarization combination the intensity arises from a mixture of water species in a "weak hydrogen-bonded" or "liquidlike" environment (~3400 cm^{-1} contribution) and of water species forming somewhat stronger hydrogen bonds (~3250 cm^{-1} contribution). However, in the ppp spectra for both the $C_{12}E_4$ and $C_{12}E_8$, a clear band centered at around 3130 cm^{-1} is seen, which is even lower than the center frequency observed in ice. This intensity at such low frequency is indicative of a water species forming particularly strong hydrogen bonds in a tetrahedrally coordinated structure similar to that observed in bulk ice. This band may also be present in the ssp spectra, but if so it is weak and convoluted with the tail of the stronger peak present at higher frequency.

Keeping in mind that VSFS can only detect molecules with a preferred orientation, the fact that such strong bands are observed in the spectra signify that the EO chains induce an ordering of the hydrating water molecules, despite themselves apparently being disordered.[70] Moreover, it is noted that in the literature a clathrate-like water structure around the poly(ethylene oxide) headgroup, including hydrogen bonding to the ether oxygen, has been proposed.[68,71] The VSFS spectra shown here provide direct spectroscopic support for such a hydration model where the strong hydrogen bonding found in a typical clathrate is the dominant feature of the water molecules observed in the spectra. Nonetheless, it is important to note that different water species of varying strength and coordination participate in the hydration of the EO groups and that a significant portion of the water molecules present in the headgroup region with a preferred orientation were found to be forming weak hydrogen bonds in a liquidlike state. The temperature and concentration dependence of the interaction between poly(ethylene oxide) surfactants and water will be presented in a separate publication.

Examining the sps and ppp spectra of Figure 6a,b, we see that a now familiar band appears centered at ~3570 cm^{-1}. This broad and strong peak is similar to that found for the other surfactants studied, assigned to the OH stretching of water molecules in close proximity to the liquid expanded hydrocarbon phase. It is observed that the intensity of this band for both the

(70) Bain, C. D. *J. Chem. Soc., Faraday Trans.* **1995**, *91*, 1281−1296.

(71) Kjellander, R.; Florin, E. *J. Chem. Soc., Faraday Trans. 1* **1981**, *77*, 2053−2077.

$C_{12}E_4$ and $C_{12}E_8$ have comparable intensities, being only slightly lower for the latter. On the basis of the area per molecule for the $C_{12}E_8$, this "non-hydrogen-bonded" band would be expected to be the largest. However, the terminal sections of the EO headgroup, having a more polymer-like behavior with increasing number of EO groups,[59] reduce the available space between the surfactant headgroups. Moreover, the higher degree of disorder in the liquid expanded phase may be responsible for the broadening of the band in the sps spectrum, as the boundary between the hydrocarbon tails and the underlying water becomes less well defined. It is interesting to note that in the ssp spectra a pronounced minimum is observed in the SF intensity at ~3570 cm^{-1}; however, at higher frequencies (~3700 cm^{-1}) a band of not negligible intensity is detected. The significance of this band will be discussed in the following section.

To facilitate comparison of the spectra taken under the same polarization conditions for the different systems, further figures are available in the Supporting Information. For example, all the spectra taken in sps polarization for the different surface films are plotted on the same figure with the same scale.

Orientational Analysis. The spectra at different polarization combinations provide the opportunity to extract information about the average orientation of the various vibrations scrutinized above. In the case of pure water, only the sharp and strong peak, unambiguously assigned to the free OH, has been used to calculate the average orientation of OH bonds that protrude into the gas phase. Using the other broader and less well defined bands, like the ones observed in the surfactant systems, to perform an orientational analysis of the contributing water species is far more delicate and prone to misinterpretations, since the exact number of species is still not clear, let alone their molecular symmetry or character responsible for the measured intensity. However, in the particular case of the "non-hydrogen-bonded" band repeatedly observed at high frequencies in all the spectra shown, the fact that the signal intensity was significantly higher in the sps and ppp than in the ssp polarization combination spectra can be used to obtain more information about the nature of this water species.

To perform the orientational analysis, it is necessary to have information about the molecular hyperpolarizability tensor elements $\beta^{(2)}_{\alpha\beta\gamma}$ of the water molecule. The nonvanishing tensor elements can be directly obtained considering the molecular C_{2v} symmetry group of water, which has proven to be an accurate approximation in the whole OH stretching range for coupled OH vibrations.[48,72] For the symmetric stretching mode, these elements are $\beta^{(2)}_{aac}$, $\beta^{(2)}_{bbc}$, and $\beta^{(2)}_{ccc}$, while for the asymmetric stretching mode only one independent element remains: $\beta^{(2)}_{aca} = \beta^{(2)}_{caa}$. In the molecular fixed coordinates of water the *c* axis is along the principal axis of symmetry (C_2), the *a* axis is along the plane formed by the H−O−H atoms, and the *b* axis is perpendicular to the *ac* plane (see Figure 8a). Another symmetry type that should be taken into account is the one involved in the uncoupled OH vibrations, such as the "free OH". In this case, the OH bond is assumed to have $C_{\infty v}$ symmetry, which reduces the $\beta^{(2)}_{\alpha\beta\gamma}$ matrix to only two independent elements: $\beta^{(2)}_{aac} = \beta^{(2)}_{bbc}$ and $\beta^{(2)}_{ccc}$ (for $C_{\infty v}$ the *c* axis follows the OH bond as shown in Figure 8b). To determine the net orientation, it is necessary to know the relative values between the different nonzero hyperpolarizability tensor elements. For the C_{2v} symmetric stretching mode these relative values are 0.69 and 0.41 for $\beta^{(2)}_{ccc}/\beta^{(2)}_{aac}$ and $\beta^{(2)}_{bbc}/\beta^{(2)}_{aac}$, respectively (the ratio for the C_{2v} asymmetric stretching mode is trivial). For the uncoupled mode under $C_{\infty v}$ symmetry, the ratio $\beta^{(2)}_{aac}/\beta^{(2)}_{ccc} = 0.32$. These values were estimated from the Raman polarizability tensor components ($\alpha_{\alpha\beta}$) of water vapor[73,74] (Raman polarizability derivatives are generally less sensitive to the environment[33] than IR transition moments and hence readily transferable).

The $\beta^{(2)}_{\alpha\beta\gamma}$ values in molecular coordinates are then first transformed into the laboratory fixed coordinate system using the Euler rotation transformation matrix and then finally orientationally averaged to obtain the tensor elements of the second-order nonlinear susceptibility ($\chi^{(2)}_{IJK}$), following a procedure described in detail elsewhere.[20] Only averaging over the azimuthal (ψ) Euler angle was performed (rotationally isotropic in the surface plane). The tilt (θ) and twist (ϕ) angle dependence was explicitly left as variables in the final susceptibility expressions. In the calculation of the Fresnel factors, which are needed for the derivation of the final simulated sum frequency curves, the values for pure water were used for the refractive indexes for the condensed bulk phase ($n_{2(SFG)} = 1.337$, $n_{2(vis)} = 1.333$, and $n_{2(IR)} = 1.15 + 0.11i$ at 3600 cm^{-1}),[75] while those of the interface were set to $n'_{SFG} = n'_{vis} = n'_{IR} = 1.20$, which are in close agreement to those proposed by Zhuang et al.[23] for the calculation of the orientation of the CN headgroup of a Langmuir monolayer. The vapor bulk values were trivially set to 1. The shapes of the curves, in particular for the C_{2v} asymmetric stretching mode, were found to be largely independent of the actual values chosen for the interfacial refractive indexes. The general conclusions were seen to remain valid for values of n' ranging from 1.1 to 1.5.

In Figure 7, the theoretical curves for the polarization intensity ratios ssp/ppp, ssp/sps, and sps/ppp are shown as a function of the tilt (θ) and specific twist (ϕ) angles (see Figure 8), where a δ distribution for both θ and ϕ was assumed. The shape of the curves differs significantly depending on the molecular symmetry considered. For the uncoupled OH stretching case only the tilt angle (θ) dependence is shown, since the twist angle carries no physical significance under the $C_{\infty v}$ molecular symmetry assumption (Figure 8). Even without performing a proper fitting analysis of the experimental spectra of the surfactant systems studied above, it is obvious that the intensity of the so-called "non-hydrogen-bonded" band in the sps and ppp spectra is always noticeably higher than that obtained for the corresponding ssp spectrum, where a pronounced minimum is observed instead. That is, the ratios I_{ssp}/I_{ppp} and I_{ssp}/I_{sps} are always < 1. It can be seen from Figure 7 that this condition can only be met for water molecules having C_{2v} symmetry with an asymmetric character, since for C_{2v} symmetric and $C_{\infty v}$ cases the experimental ratio does not, in most occasions, even intersect any of the theoretical curves. Moreover, it is also apparent that the intensity ratio between the sps and ppp polarization combinations for this band is close to 1. For such a ratio the obtained tilt ranges from 30° to ~50° from the surface normal, for twist angles spanning from 0° to ~60°, where these last are higher for increasing tilts. These numbers should be

(72) Fischer, W. B.; Eysel, H.-H. *J. Mol. Struct.* **1997**, *415*, 249−257.
(73) Murphy, W. F. *Mol. Phys.* **1978**, *36*, 727−732.
(74) Avila, G.; Fernandez, J. M.; Mate, B.; Tejeda, G.; Montero, S. *J. Mol. Spectrosc.* **1999**, *196*, 77−92.
(75) Hale, G. M.; Querry, M. R. *Appl. Opt.* **1973**, *12*, 555−563.

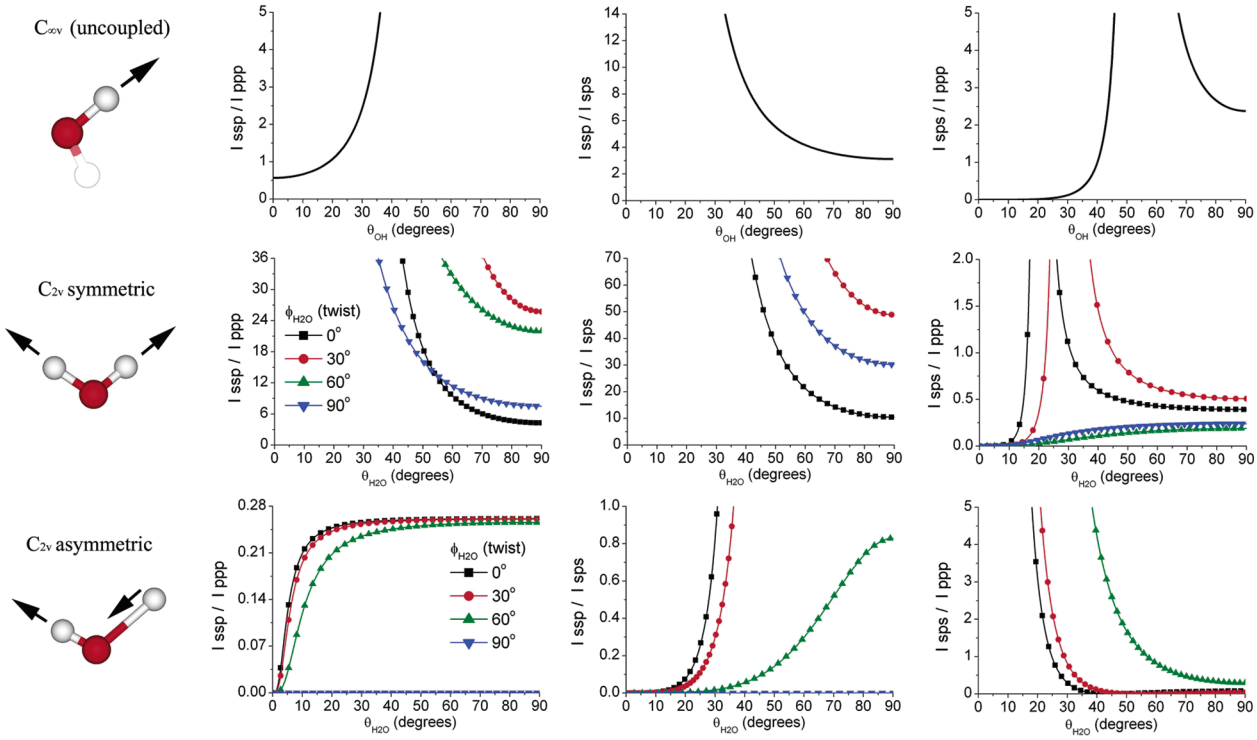

Figure 7. Calculated curves for the relative intensity for three different polarization combination ratios (I_{ssp}/I_{ppp}, I_{ssp}/I_{sps}, and I_{sps}/I_{ppp}) of the OH stretching bands of water assuming an uncoupled OH vibration ($C_{\infty v}$) and symmetric and asymmetric stretches of water (C_{2v}). The sets of curves for the C_{2v} vibrations are expressed as a function of the tilt (θ) and twist (ϕ) angles. Only the C_{2v} asymmetric curves comply with the experimental results obtained for the "non-hydrogen-bonded" band, where I_{ssp} is significantly lower than I_{sps} and I_{ppp}.

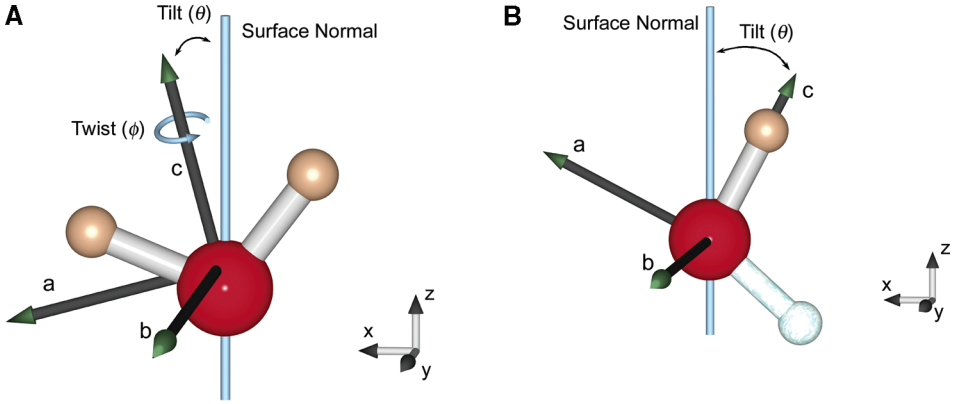

Figure 8. (a) Molecular model for a C_{2v} symmetry water molecule. The molecular coordinates axes (a,b,c) and surface coordinates axes (x,y,z) are shown for reference. The c axis is along the C_2 principal axis of symmetry, while the origin is at the center of mass. The tilt (θ) corresponds to the angle between the molecular c axis and the surface normal, while the twist (ϕ) refers to the angle between the a axis and the cz plane (in the sketch $\phi = 0°$). All possible combinations of angles for θ and ϕ obtained from the orientation analysis of the "non-hydrogen-bonded" band indicate that both hydrogen atoms always lie in the upper quadrants of the surface coordinate system. (b) Molecular model for the $C_{\infty v}$ symmetry uncoupled OH vibration of a water molecule.

seen as just rough estimates as a δ distribution of angles was assumed in the calculation, implying that all water molecules responsible for this band have exactly the same orientation, which is inconsistent with the broad nature of the "non-hydrogen-bonded" band. A more realistic Gaussian function for the distribution of angles was also evaluated, showing very similar trends (data not shown).

The net polar orientation of the water molecules responsible for this band (i.e., whether the hydrogen atoms point toward the bulk liquid or the hydrocarbon tails) cannot be explicitly obtained from the experimental data, since phase measurements were not performed.[14] However, it can be directly inferred from the position of the band and the combination of tilt and twist angles from the orientation analysis that both hydrogen atoms must indeed be directed toward the surfactant hydrocarbon tails and as such do not participate in hydrogen bonds with other water molecules. These water molecules are nonetheless not completely free of H-bonds, since this preferred orientation necessarily leaves the lone-pair electrons of the oxygen atom facing toward the bulk liquid, where they could act as hydrogen bond acceptors. It has been shown that the red shift in frequency of the OH stretching vibration for water dimers due to an acceptor hydrogen bond is relatively small;[76,77] this fact, coupled with the fact that the hydrogen atoms are vibrating toward the oily region rather than in air, seems sufficient to explain the

(76) Nelander, B. *J. Chem. Phys.* **1988**, *88*, 5254−5256.
(77) Bouteiller, Y.; Perchard, J. P. *Chem. Phys.* **2004**, *305*, 1−12.

shift of ~100 cm^{-1} from the stretching vibration of gas-phase water.

Measurements from other groups[15,78] have shown that for a pure hydrocarbon/water interface (where the structure is not perturbed by the presence of headgroups) a band equivalent to that of the free OH at the water/air interface is observed in the ssp polarization combination. That is to say, one of the hydrogen atoms points toward the hydrocarbon, while the other is directed toward bulk water and participates in hydrogen bonding (Figure 8b). It must be stressed that the "nondonor" band discussed in the preceding paragraph should not be confused with this band. There is a significant difference in wavenumber, and the orientational analysis definitively precludes such a structure. However, since the water molecules studied here are also in contact with a hydrocarbon region, it is apposite to wonder why this band is not observed here. In fact, a close examination of all the ssp spectra presented (Figures 4, 5, and 6) reveals that a weak intensity is observed at frequencies comparable to those of the free OH of water (~3700 cm^{-1}) but with a significantly broader bandwidth, suggesting heterogeneity in the interactions with neighboring molecules.

The reason for the "nondonor" orientation to be favored over the uncoupled "free" orientation for nonionic surfactant monolayers at the air/water interface is not entirely obvious, and we can only speculate as to its origin. Clearly the main difference to the case of a hydrocarbon/water interface is the presence of hydrophilic groups which alternate with hydrophobic patches from the tail region over short distances. Thus these results imply that the free OH configuration is the result of a structured layer at the interface, involving a certain number of neighboring water molecules. When these domains are perturbed by the polar headgroups the structuring is lost or significantly perturbed, and the preferred orientation of the "nondonor" molecules is seen to arise, probably due to weak interactions between the hydrocarbon tails and water.

What is remarkable in the observation of nondonors is that the energy cost of sacrificing a hydrogen bond is very large and the free energy of mixing with headgroups in the surface alone is hardly likely to compensate for this. *The entropically costly structuring of water molecules in the proximity of the free OH, however, would not be as severe for the nondonor state*. Hence, the local cost in free energy upon the loss of hydrogen bonding could be compensated by the entropy gain upon release of oriented water molecules. This is a very interesting finding as the state of the water molecules in the proximity of hydrophobic interfaces and the effect of surfactant adsorption upon the state of these molecules is of great general relevance.

Summary and Conclusion

Vibrational sum frequency spectroscopy using the polarization combinations ssp, ppp, and sps has been used to determine the structure of water at the liquid/air interface of solutions of soluble nonionic surfactants forming a liquid-expanded phase. Remarkable differences between these surfaces and the pure water surface in the OH stretching range of water were observed, reflecting the very distinct nature of the water structure at these interfaces. Moreover, comparing the different amphiphilic molecules investigated, we found the spectral features on the low frequency side to be strongly dependent on the surfactant headgroup and associated with water molecules participating in the hydration of the headgroup.

For decanol and the surfactants C_{10}Glucoside and C_{10}-Maltoside, the intensity observed in the VSF spectra at low frequencies also involves the stretching vibrations of the hydroxyl groups present in the respective headgroups. For the particular case of the sugar surfactants, it was inferred that the water molecules detected forming the hydration shell were a direct consequence of the preferred orientation of the headgroup rings. Additionally, the strength of the hydrogen bonds in the hydration shell was found to be strong and similar to those observed for tetrahedrally coordinated water molecules in ice. The poly(ethylene oxide) headgroup, on the other hand, despite being itself disordered was shown to induce a significant ordering and structuring of water at the surface. Most of this water was found to form relatively strong hydrogen bonds, including a population of molecules forming particularly strong bonds, at frequencies lower than those observed in tetrahedrally coordinated water molecules in ice. This observation supports the creation of a clathrate-like water structure around the poly-(ethylene oxide) chains.

Another relevant feature observed in the high frequency region of the ppp and sps spectra and common to all surfactant systems studied was a band assigned to water molecules vibrating in close proximity to the hydrocarbon tails and very weakly interacting with neighboring H_2O molecules. From the orientational analysis, it was concluded that this intensity mainly originates from asymmetric vibrations of water molecules with C_{2v} symmetry. The range of possible angles for the twist and tilt, despite being broad, was seen to be consistent with both hydrogen atoms preferentially ordered toward the hydrocarbon tails and not forming hydrogen bonds (nondonor molecules).

In contrast to the VSF spectra of the neat water surface and of water/oil interfaces,[15,78] the surfactant systems studied in this report do not show the sharp peak centered at ~3700 cm^{-1}, assigned to the free OH or uncoupled stretching vibration of an OH bond protruding out into the gas, or oil phase, respectively. This is not entirely surprising, since the polar headgroups are expected to disrupt the surface structure. These facts entail that the sharp free OH intensity is the result of the structuring and cooperative interactions of a certain number of water molecules in the underlying liquid. In the presence of a polar group, *these domains are perturbed* and the sharp free OH signal is lost. Nonetheless, water molecules with a preferred orientation are still observed in direct contact to the hydrocarbon tails. We speculate that the enthalpically unfavorable nondonor orientation is compensated entropically by the release of oriented water molecules.

These studies provide novel information about the hydration state of nonionic surfactants and interaction between water and hydrocarbon tails. The different types of headgroups used here have relevance in biochemistry, which opens up the possibility of using VSFS to investigate and increase our understanding of the role of water in important biological and technological issues, including temperature-induced phase inversion of microemulsions, formation of inert protein-repellent coatings for bioassays, as well as reaction and binding conditions at glycolipid and glycoprotein surfaces.

(78) Du, Q.; Freysz, E.; Shen, Y. R. *Science* **1994**, *264*, 826−828.

Acknowledgment. Financial support from the Swedish Research Council (VR), the Swedish Research Council for Engineering Sciences (TFR), and the Swedish Foundation for Strategic Research (SSF) is gratefully acknowledged. We thank Dr. Steve Baldelli (University of Houston) for valuable discussions and encouragement.

Supporting Information Available: VSF spectra for the polarization combination ssp, ppp, and sps of aqueous solution of C10Glucoside, C10Maltoside, 1-Decanol, and C12E4. This material is available free of charge via the Internet at http://pubs.acs.org.

JA053289Z